Isotopic composition of cosmic-ray sources

I. V. MOSKALENKO[1,2], A. W. STRONG[3], AND T. A. PORTER[4]

[1] *Hansen Experimental Physics Laboratory, Stanford University, Stanford, CA 94305, U.S.A.*

[2] *Kavli Institut for Particle Astrophysics and Cosmology, Stanford University, CA 94309, U.S.A.*

[3] *Max-Planck Institut für extraterrestrische Physik, Garching, Germany*

[4] *Santa Cruz Institute for Particle Physics, University of California, Santa Cruz, CA 95064, U.S.A.*

imos@stanford.edu

Abstract: We use the GALPROP code and the Advanced Composition Explorer (ACE) data to derive the cosmic ray (CR) isotopic composition at the sources. The composition is derived for two propagation models, diffusive reacceleration and plain diffusion. We show that the compositions derived assuming these two propagation models are different. We also compare the isotopic composition at the sources with the latest solar composition.

Introduction

CR source abundances are normally derived using the leaky-box or weighted slab approximations to interstellar propagation. While this is a valid procedure under some conditions (see [20] for a review) at least for stable nuclei, there are reasons for preferring a more physically-based approach. For example, the distribution of CR sources (e.g., supernova remnants) in the Galaxy is probably peaked towards the inner Galaxy, as recently supported by γ-ray observations [19], and this affects the path-length distribution in a way that requires a detailed spatial propagation model. Another example is the effect of diffusive reacceleration, which is probably important in reproducing the energy-dependence of the secondary/primary ratios, and this will also affect the derivation of source abundances. The parameters of the models used to derive the source abundances should also be compatible with other observational constraints from gas surveys, γ-rays, synchrotron and so on [17, 12, 18, 19].

In this paper, we use the GALPROP CR propagation code [16] to derive source isotopic abundances from ACE data. Both the astrophysical model and the cross-sections play a key role in the uncertainties in such a computation; here we present preliminary results, reserving detailed discussion to a future journal paper.

Method

The GALPROP code[1] computes a complete network of primary, secondary and tertiary production starting from input source abundances, as described in [16, 18, 14]. The nuclear reaction network is built using the Nuclear Data Sheets. The isotopic cross-section database is built using the extensive T16 Los Alamos compilation of the cross-sections [8] and modern nuclear codes CEM2k and LAQGSM [9]. The most important isotopic production cross-sections (2H, 3H, 3He, Li, Be, B, Al, Cl, Sc, Ti, V, and Mn) are calculated using our fits to major production channels [11, 12]. Other cross-sections are calculated using phenomenological approximations by Webber et al. [21] (code WNEWTR.FOR versions of 1993 and 2003) and/or Silberberg and Tsao [15] (code YIELDX_011000.FOR version of 2000) renormalized to the data where it exists. The K-capture and electron stripping processes are included, where a nucleus with one electron is considered a separate species because of the difference in lifetime.

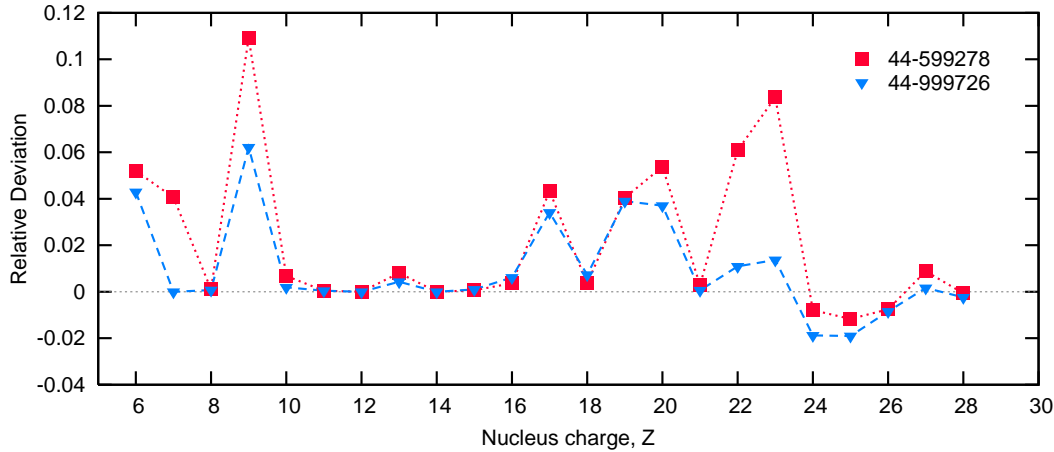
1. http://galprop.stanford.edu

Figure 1: Quality of the fit: fractional deviations of propagated elemental abundances from ACE observations [22].

The propagation equation is solved numerically starting with the heaviest nucleus (i.e., ^{64}Ni), computing all the resulting secondary source functions, and then processes the nuclei with $A - 1$. The procedure is repeated down to $A = 1$. To account for some special β^--decay cases (e.g., ^{10}Be→^{10}B) the whole loop is repeated twice. The current version employs a full three-dimensional spatial grid for all CR species, but for the purposes of this study the 2D cylindrically symmetrical option is sufficient.

To calculate the isotopic source abundance, we adopt an iterative procedure, which uses the deviations of calculated propagated abundances from abundances observed by ACE at 200 MeV/nucleon [22] to correct the source abundances until a good fit is obtained. In practice very good agreement (a few %) can be obtained in about ten iterations. The basic parameters of the propagation model are based on fitting the energy-dependence of the B/C ratio, for which the best data are available and cross-sections best known. The parameters are given in [14]. Solar modulation is calculated using the force-field approximation [6]. The modulation potential $\Phi = 450$ MV corresponds approximately to the period of solar activity when the data were collected. An analysis of source abundances of isotopes of P, S, Ar, Ca is given in [13]. Discussion of propagation of Li, Be, B in the same models can be found in [4].

Results

We applied the technique to the plain diffusion and the diffusive reacceleration models as described in [14]. We consider here only the effect of the propagation; the effect of a more realistic source distribution will be considered elsewhere (Moskalenko et al., in preparation). The quality of the fit can be judged from Figure 1, which shows the propagated abundances of elements minus abundances measured by ACE. The fitted values are *isotopic* abundances while the plot shows fractional deviations of *elemental* abundances for clarity. It can be seen that the propagated abundances are reproduced with a maximum error of 5% (10% for the least abundant elements).

The deviations from "0" are mainly due to the errors in the cross sections. It can be illustrated using Carbon as an example. The propagated abundance of ^{12}C agrees perfectly with the data since the source abundance of this isotope is adjusted iteratively. The isotopic abundance of ^{13}C cannot be adjusted in the same way since it is already zero (from the fitting), but it is overproduced due to the spallation of heavier nuclei (see discussion in [12]). The entire excess of Carbon $\sim$5% is due to the overproduction of ^{13}C during the CR propagation. Similarly, F is entirely secondary and the excess is due to the cross-section uncertainties.
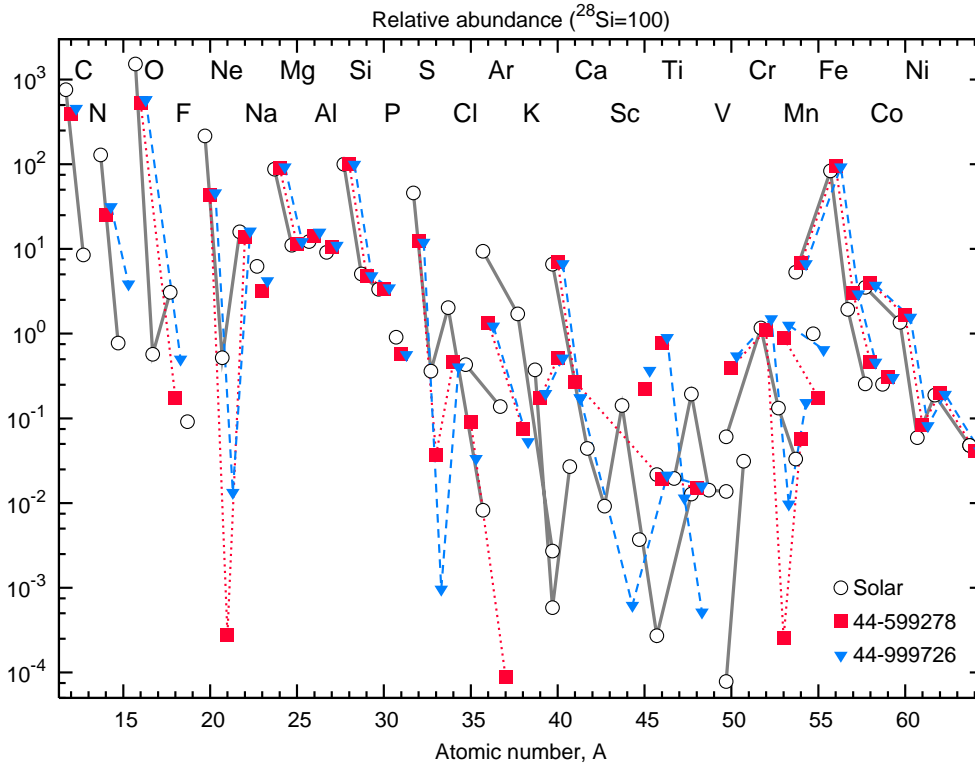
Figure 2: Source isotopic abundances. Circles: solar system abundances [7], squares: diffusive reacceleration model, triangles: plain diffusion model. Isotopes of the same element are connected by the lines. The lowest values are included to show the solar abundances; in these cases the CR source abundances are not always reliable.

The isotopic abundances ($A > 6$) for the two models are compared with latest solar abundances from [7] in Figure 2. We do not show the isotopes where the source abundances are extremely small ($<10^{-4}$) because the accuracy of the cross sections is insufficient in these cases. The derived source isotopic abundances generally agree better with the latest solar abundances from [7], especially the iron group, than with the earlier version of solar abundances by Anders and Grevesse [1]. Still, the source abundances derived in both models are underabundant relative to solar in many cases, as is well known, e.g. C, N, O, Ne, S, Cl, Ar, Sc. In other cases we confirm the remarkable agreement with solar: Na, ^{40}Ca, Mg, Al, Si, ^{52}Cr, Fe, Co, Ni. In many cases a good agreement with solar abundances is apparent also for isotopes with large

proportion of secondary production: ^{22}Ne, ^{23}Na, ^{25,26}Mg, ^{27}Al, ^{29,30}Si, ^{31}P, ^{54,57,58}Fe, ^{59}Co, ^{61}Ni.

The abundances are very much dependent on the isotopic production cross sections which are uncertain to a large degree, e.g., F, P, Ar, K, Sc, Ti, V (see discussion in [12]). The source abundance of ^{16}O, which is mostly primary, is less than solar by a significant factor. The fragmentation cross sections are known much better than the isotopic production cross sections, so this result is rather robust. Similarly, we confirm that the source abundances of ^{14}N and ^{20}Ne are a factor of 5–6 below solar. The well-known excess ^{22}Ne/^{20}Ne (see, e.g., [2]) is also evident. Subject to further verification and the accuracy of the production cross sections, the study shows that many isotopes in CR are mostly secondary, ^{13}C, ^{17}O, ^{21}Ne, ^{33,34,36}S, ^{37}Cl, ^{38,40}Ar, ^{41}K, ^{42,43,44}Ca, ^{53}Cr. This is in ad-

dition to Li, Be, B, F, P, Sc, Ti, V that have been discussed in the literature for a long time. There are also a few cases where the model predictions are different from each other, e.g., ^{15}N, ^{18}O, ^{21}Ne, ^{33}S, ^{55}Mn, and some others. These differences can be used to constrain or rule out some propagation models.

Interestingly, radioactive ^{41}Ca and ^{53}Mn appear to be significantly present in the sources. Radioactive ^{41}Ca is a K-capture isotope that decays (to ^{41}K) with a period $\tau_{1/2} = 1.03 \times 10^5$ yr and has a negligible abundance in the solar system. A similar case is radioactive ^{53}Mn, another K-capture isotope that decays to ^{53}Cr with a period $\tau_{1/2} = 3.74 \times 10^6$ yr. Their abundances can be used to constrain the CR acceleration time scale.

Conclusion

This is the first time that a 'realistic' (i.e. full spatial- and energy-dependence) propagation model has been used to derive isotopic source abundances for a full range of CR nuclei. As is well-known, the elements with low first ionization potential (FIP) appear to be more abundant in CR sources relative to the high-FIP elements, when compared with the solar system material. This might imply that the source material includes the atmospheres of stars with temperatures $\sim 10^4$ K [3]. A strong correlation between FIP and volatility (most of low-FIP elements are refractory while high-FIP elements are volatile) suggests that CRs may also originate in the interstellar dust, pre-accelerated by shock waves [10, 5]. CR data tend to prefer volatility over FIP, but uncertainties in the derived source abundances have prevented an unambiguous solution.

The analysis presented in this paper shows that the radioactive ^{41}Ca and ^{53}Mn appear to be significantly present in the sources. This may be used to study the CR acceleration timescale and seems to give more support to the volatility hypothesis. The detailed discussion and error analysis will be presented in a forthcoming journal publication.

References

[1] Anders, E., & Grevesse, M., Geochim. Cosmochin. Acta **53**, 197 (1989).

[2] Binns, W. R., et al., ApJ **634**, 351 (2005).

[3] Cassé, M., & Goret, P., ApJ **221**, 703 (1978).

[4] de Nolfo, G. A., et al., Adv. Space Res. **38**, 1558 (2006).

[5] Epstein, R. I., MNRAS **193**, 723 (1980).

[6] Gleeson, L. J., & Axford, W. I., ApJ **154**, 1011 (1968).

[7] Lodders, K., ApJ **591**, 1220 (2003).

[8] Mashnik, S. G., et al., arXiv: nucl-th/9812071 (1998).

[9] Mashnik, S. G., et al., Adv. Space Res. **34**, 1288 (2004).

[10] Meyer, J.-P., Drury, L. O'C., & Ellison, D. C., ApJ **487**, 182 (1997).

[11] Moskalenko, I. V., Mashnik, S. G., & Strong, A. W., Proc. 27th ICRC (Hamburg), 1836 (2001).

[12] Moskalenko, I. V., Strong, A. W., Mashnik, S. G., & Ormes, J. F., ApJ **586**, 1050 (2003).

[13] Ogliore, R. C., et al., Proc. 30th ICRC (Merida), paper # 698 (2007).

[14] Ptuskin, V. S., Moskalenko, I. V., Jones, F. C., Strong, A. W., & Zirakashvili, V. N., ApJ **642**, 902 (2006).

[15] Silberberg, R., Tsao, C. H., & Barghouty, A. F., ApJ **501**, 911 (1998).

[16] Strong, A. W., & Moskalenko, I. V., ApJ **509**, 212 (1998).

[17] Strong, A. W., Moskalenko, I. V., & Reimer, O., ApJ **537**, 763 (2000).

[18] Strong, A. W., Moskalenko, I. V., & Reimer, O., ApJ **613**, 962 (2004).

[19] Strong, A. W., Moskalenko, I. V., Digel, S., Reimer, O., & Diehl, R., A&A **422**, L47 (2004).

[20] Strong, A. W., Moskalenko, I. V., & Ptuskin, V. S., Ann. Rev. Nucl. Part. Sci. **57**, 285 (2007).

[21] Webber, W. R., Kish, J. C., & Schrier, D. A., Phys. Rev. C **41**, 566 (1990).

[22] Wiedenbeck, M. E., et al., Spa. Sci. Rev. **99**, 15 (2001).